

Effect of High Pressure Heat Treatment on the Phase Transformation Dynamics of $\alpha+\gamma_2\rightarrow\beta$ in Cu-Al Alloy

Dong Cao^a 

^a*Xi'an Aeronautical University, Xi'an 710077, China*

Received: October 15, 2019; Revised: February 29, 2020; Accepted: March 7, 2020.

In this paper, high pressure heat treatment for Cu-Al alloy is carried out at the pressure of 5GPa and the heating temperature of 700°C for 15 minutes. The phase transformation temperature and time of $\alpha+\gamma_2\rightarrow\beta$ in Cu-Al alloy are measured before and after 5GPa pressure treatment with the help of differential scanning calorimeter (DSC). The activation energy and Avrami exponent for phase transformation are also calculated. Based on the measurement, calculation and observation of the alloy's microstructure, the effect of 5GPa pressure treatment on the phase transformation of $\alpha+\gamma_2\rightarrow\beta$ in Cu-Al alloy is discussed thoroughly. The results show that 5GPa pressure treatment can decrease the phase transformation temperature and activation energy of $\alpha+\gamma_2\rightarrow\beta$ in the alloy. It can also shorten the phase transformation time while increasing the Avrami exponent. These are beneficial to the phase transformation of $\alpha+\gamma_2\rightarrow\beta$ in Cu-Al alloy since the microstructure of Cu-Al alloy gets refined and dislocation density increases after the high pressure heat treatment. Note that the high pressure process has less effect on the mechanism of phase transformation.

Keywords: *Cu-Al alloy; 5GPa pressure treatment; solid state transformation of $\alpha+\gamma_2\rightarrow\beta$; microstructure.*

1. Introduction

It is well known that copper alloy has high electrical conductivity, high thermal conductivity, and good corrosion resistance. Thus, it has been widely applied in many fields, such as electricity, electrical and aviation. However, the grain of copper alloy grows easily which will reduce the strength of copper alloy and thus limit the application of this material¹. Fortunately, high pressure treatment can promote nucleation, suppress atomic transport, and inhibit the growth of grain, thus has the potential to gain fine-grained alloy²⁻⁴. Therefore, a lot of attention has been paid on the effect of high pressure treatment on metal materials to ameliorate alloy microstructure and its performance⁵⁻⁷. Recent researches show that high pressure treatment is beneficial to obtain the refined microstructure of Cu-Al alloy and thus enhance the strength of alloy⁸. Since some application components made of Cu-Al alloy usually work at a certain temperature, the solid state phase transformation will occur inevitably with the increase of temperature. The microstructure and properties of Cu-Al alloy will be badly influenced accordingly. However, it is still unclear how will the high pressure treatment affect the solid state phase transformation of Cu-Al alloy.

A lot of research has been done on solid state phase transformation of metal materials. Some works focus on the evolution of phase^{9,10} and some works study the solid state phase transformation via phase field method¹¹⁻¹³. However, the phase field method does not involve some important phase transformation parameters, such as temperature,

time, activation energy, and Avrami exponent. Actually, the temperature and time for phase transformation are the key parameters to characterize the structure of metal materials. Moreover, the activation energy and Avrami exponent are two important dynamic parameters to reflect the behavior of solid state phase transformation. Therefore, it has some practical significance to investigate the aforementioned parameters during the solid state phase transformation. Recently, the effect of high pressure treatment on solid state phase transformation of metal materials has already been studied in the literatures¹⁴⁻¹⁶, which can provide some quantitative descriptions or results for the phase transformation parameters. However, the reason for why high pressure treatment affects the phase transformation parameters has not been clearly analyzed.

Based on these observations, in this paper we consider the status of Cu-Al alloy before and after the high pressure treatment, and measure the changes of phase transformation temperature, time, activation energy, and Avrami exponent during the following heating process. We also obtain the relationship between phase transformation temperature, time, and activation energy. Specially, we carefully study the effect of high pressure treatment on dynamics of solid state phase transformation of Cu-Al alloy during the following heating process. The results can provide some references to figure out the effect of high pressure treatment on the phase transformation of Cu-Al alloy, and also predict the structure of Cu-Al alloy during the heating process. Moreover, our work will enrich the application of high-pressure research to the field of copper alloy.

*e-mail: caodong@xaau.edu.cn

2. Experiment

The materials to be tested were Cu-Al alloys which consist of 88.24% Cu, 11.76% Al, and 0.63% other elements (mass fraction, %). The specimens were firstly smelted into the vacuum intermediate frequency induction furnace at about 1150°C and maintained for 15 minutes. Then, the specimens were casted into cylindrical billets in graphite mold. The cylindrical billets were finally processed into samples of size $\Phi 5\text{mm} \times 2\text{mm}$. The experiments for high pressure treatment were performed on the six-anvil high-pressure equipment with the type of CS-IIIB. The samples were first pressurized to 5GPa and heated to 700°C, and then maintained for 15 minutes. After the above processing, the pressure was released until the samples were cooled to room temperature. Measurements utilizing differential scanning calorimeter (DSC) (Model STA449C, Jupiter, Netzsch, Germany) were carried out to analyze the status of Cu-Al alloy samples before and after the aforementioned high pressure treatment. The heating temperature was set as 700°C and the heating rate was set as $5^\circ\text{C} \cdot \text{min}^{-1}$, $10^\circ\text{C} \cdot \text{min}^{-1}$, and $20^\circ\text{C} \cdot \text{min}^{-1}$, respectively.

The phase transformation activation energy (denoted as E_c) of the sample can be calculated by the Kissinger equation¹⁷: $\ln(BT^{-2}) = -E_c(RT)^{-1} + C$, where B is the heating rate, T is the temperature, R is the gas constant, and C is a constant. The phase transformation activation energy at a certain stage (denoted as E_x) can be determined by the Deloy method¹⁸:

$$\log B = \log AE[R \cdot F(X)]^{-1} - 2.315 - 0.4567E_x(RT)^{-1},$$

where B is the heating rate, R is the gas constant, T is the temperature, X is the phase transformation volume fraction, A is the frequency factor, and $F(X)$ is the phase transformation function. When X is a constant, the term $\log AE[R \cdot F(X)]^{-1}$ is also a constant. The Avrami exponent (denoted as n) can be obtained by¹⁹: $n = 2.5T_p^2(\Delta\tau_{FWTH}E_cR^{-1})^{-1}$, where $\Delta\tau_{FWTH}$ is the width corresponding to half of the maximum DSC endothermic peak, T_p is the peak temperature for DSC

endothermic peak, E_c is the phase transformation activation energy, and R is the gas constant.

The samples were cut along the lengthwise direction, sanded, polished, and finally etched in the etching solution which is comprised of 1g $\text{FeCl}_3 + 20\text{ml HCl} + 100\text{ml H}_2\text{O}$. The microstructures and compositions of the samples were observed on the Axiovert 200MAT metalloscope, Jeol-2010 transmission electron microscope (TEM), KYKY-2800 scanning electron microscope (equipped with energy spectrum EDS), and D/MAX-rB X-ray diffractometer (with graphite monochromator and $K\alpha$ radiation).

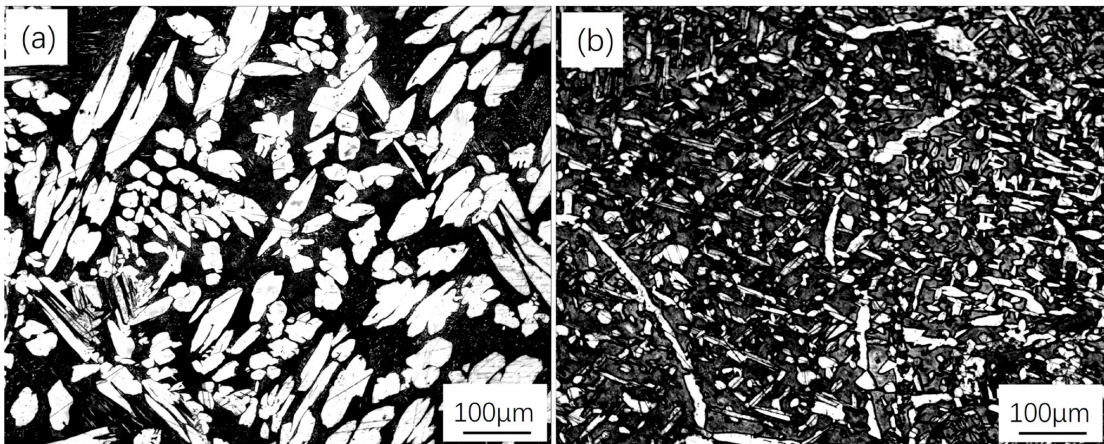
3. Results and Discussions

3.1 Microstructure

Figure 1 shows the microstructures of Cu-Al alloy before and after 5GPa pressure treatment, which are labeled as “As-cast” and “5GPa pressure treatment”, respectively. We see that the microstructures are composed of irregular white and black zones in both cases. Specially, the metallographic images reveal that the grain size after 5GPa treatment is less than that before 5GPa treatment.

The XRD diffraction pattern in Figure 2 illustrates that the alloy structure is composed of α , β and γ_2 phases, where α phase is the solid solution based on Cu, β phase is the solid solution based on AlCu_3 , and γ_2 phase is the solid solution based on Al_4Cu_9 . From the EDS analysis in Table 1, we find that the main components in both white and black zones are Cu and Al. The element content of Cu in the white zone is more than that in the black zone while the content of Al in the white zone is less than that in the black zone. Therefore, we can deduce that the white zone belongs to α phase while β and γ_2 phases mainly exist in black zone.

Moreover, it can be observed from the TEM images of Cu-Al alloy that the dislocation density increases obviously after high pressure treatment, as shown in Figure 3. High pressure treatment can bring high residual stress and strain



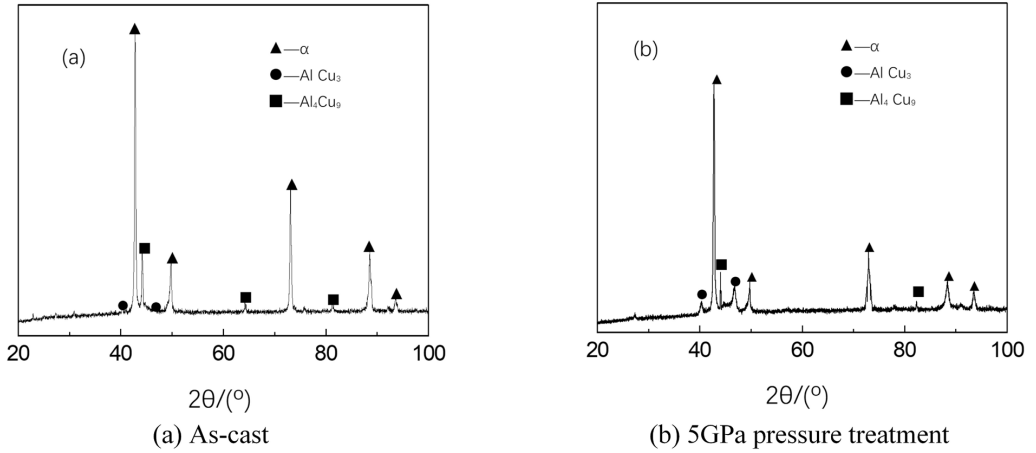
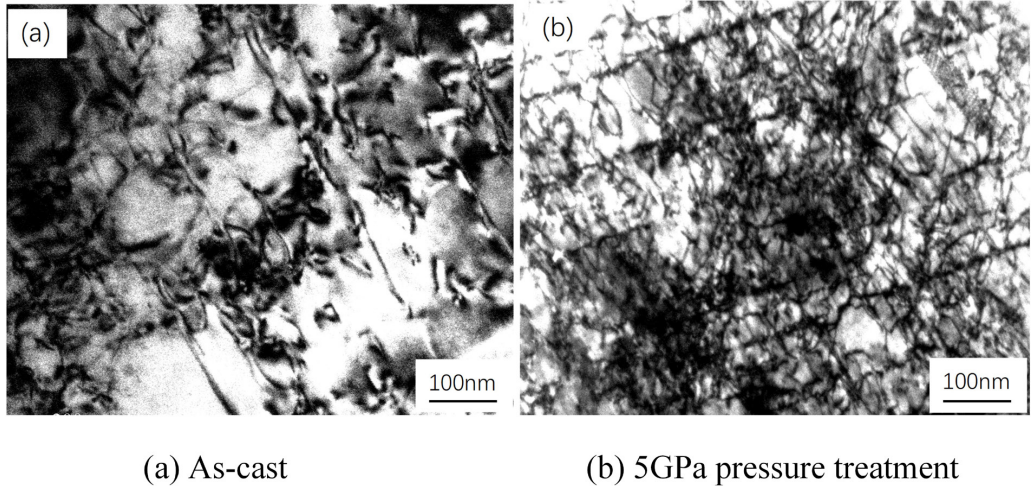
(a) As-cast

(b) 5GPa pressure treatment

Fig.1 - Microstructure of Cu-Al alloy before and after high pressure treatment

Table 1 - Micro-zone composition analyses of Cu-Al alloy before and after high pressure treatment.

Sample	Zone	Cu (wt.%)	Al (wt.%)
As-cast	White zone	90.94~91.41	8.59~9.06
	Black zone	76.85~84.26	15.74~23.15
5GPa	White zone	91.07~91.31	8.69~8.93
	Black zone	76.84~84.66	15.34~23.16

**Fig.2** - XRD patterns of Cu-Al alloy before and after high pressure treatment**Fig.3** - TEM images of Cu-Al alloy before and after high pressure treatment

in the alloy, which in turn makes the lattice deformation and further results in plenty of dislocation in the alloy. The latter provides more favorable nucleation sites for $\alpha+\gamma_2\rightarrow\beta$ phase transformation. Meanwhile, high pressure can reduce the rate of atomic transport and suppress the growth of crystal nucleus. Therefore, more refined grains of Cu-Al alloy can be obtained and higher dislocation density can be observed after high pressure treatment.

3.2 Phase transformation at constant heating rates

Figure 4 shows the DSC curves of Cu-Al alloy before and after high pressure treatment at constant heating rates of $5^\circ\text{C}\cdot\text{min}^{-1}$, $10^\circ\text{C}\cdot\text{min}^{-1}$, and $20^\circ\text{C}\cdot\text{min}^{-1}$, respectively.

One endothermic peak can be seen clearly on each DSC curve before and after high pressure treatment. Based on phase diagram of Cu-Al alloy²⁰, the peak corresponds to the solid state phase transformation in heating process, that is, $\alpha(\text{Cu}) + \gamma_2(\text{Al}_4\text{Cu}_9) \rightarrow \beta(\text{AlCu}_3)$.

The initial temperature (T_1), peak temperature (T_p), and ending temperature (T_2) for the phase transformation are defined as the temperatures at the starting point, peak point, and ending point of endothermic in the DSC curves, respectively. The transformation duration (t) is then calculated by: $t=(T_1-T_2)/B$, where B is the heating rate. Therefore, the initial temperature, peak temperature, ending temperature, and duration of the phase transformation can be deduced from the DSC curves in Figure 4 at different heating rates, which are listed in Table 2. It can be observed that the initial

Table 2 - Phase transformation temperature and duration of $\alpha+\gamma_2\rightarrow\beta$ in Cu-Al alloy before and after high pressure treatment under different heating rates.

Heating rate /°C.min ⁻¹	Initial temperature/°C		Peak temperature/°C		Ending temperature/°C		Transformation duration/s	
	As-cast	5GPa	As-cast	5GPa	As-cast	5GPa	As-cast	5GPa
5	562.47	559.59	570.56	564.11	589.83	580.68	328.32	257.88
10	564.32	560.02	574.87	567.64	592.25	582.37	167.58	134.10
20	566.49	561.07	576.47	571.52	601.36	585.41	104.61	73.02

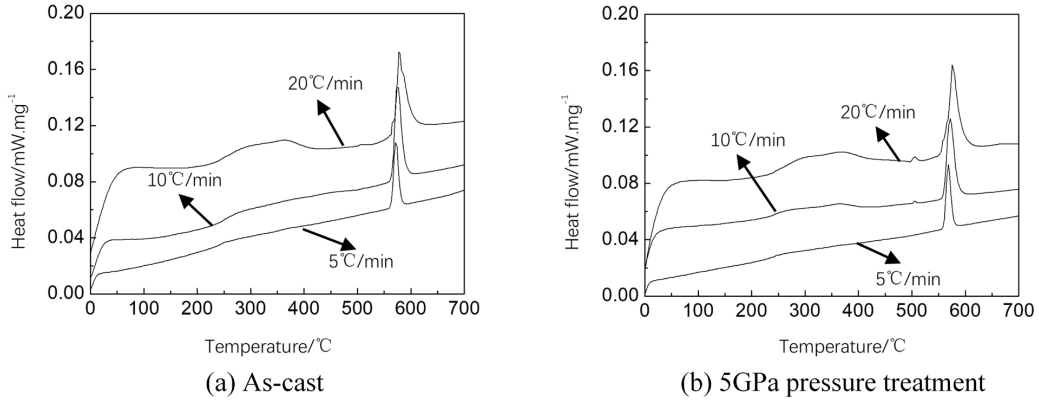


Fig. 4 - DSC curves of Cu-Al alloy before and after high pressure treatment at different heating rates

temperature, peak temperature, and ending temperature of $\alpha+\gamma_2\rightarrow\beta$ phase transformation all grow with the increase of heating rate. The Cu-Al alloy after high pressure treatment shows lower phase transformation temperature and shorter phase transformation duration than that without high pressure treatment. Taking the heating rate of $10^\circ\text{C}\cdot\text{min}^{-1}$ for an example, the phase transformation peak temperature and the phase transformation duration of the Cu-Al alloy after high pressure treatment will decrease 2.7°C and 11.9s , respectively, which reveals that the $\alpha+\gamma_2\rightarrow\beta$ phase transformation is more prone to happen during the heating process after the high pressure treatment.

3.3 Phase transition activation energy

According to the Kissinger equation: $\ln(BT^{-2}) = -E_c(RT)^{-1} + C$, the terms $\ln(BT^{-2})$ and T^{-1} for the peak values at various heating rates before and after high pressure treatment can be obtained from the results shown in Table 2, where the unit for peak temperature T is K ($K=273.15+^\circ\text{C}$). We further plot the relationship between $\ln(BT^{-2})$ and T^{-1} in Figure 5, which is close to linear variation. It shows that the Kissinger equation also subjects to linear variation and the slope is $K'=E_c/R$. According to Figure 5, the slopes K' under two cases can be calculated using the least square method. Since we have $K'=E_c/R$, the phase transformation activation energy E_c of $\alpha+\gamma_2\rightarrow\beta$ in Cu-Al alloy before and after high pressure treatment can be obtained by: $E_c=K'R$, i.e., $1296.58\text{kJ}\cdot\text{mol}^{-1}$ and $1174.85\text{kJ}\cdot\text{mol}^{-1}$, respectively. We see that the high pressure treatment can reduce the $\alpha+\gamma_2\rightarrow\beta$ phase transformation activation energy. It can be concluded that high pressure treatment can decrease the $\alpha+\gamma_2\rightarrow\beta$ phase transformation consumption barrier in the subsequent heating process and make the $\alpha+\gamma_2\rightarrow\beta$ phase transformation much easier.

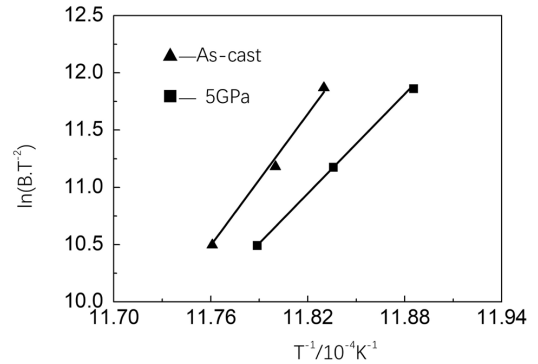
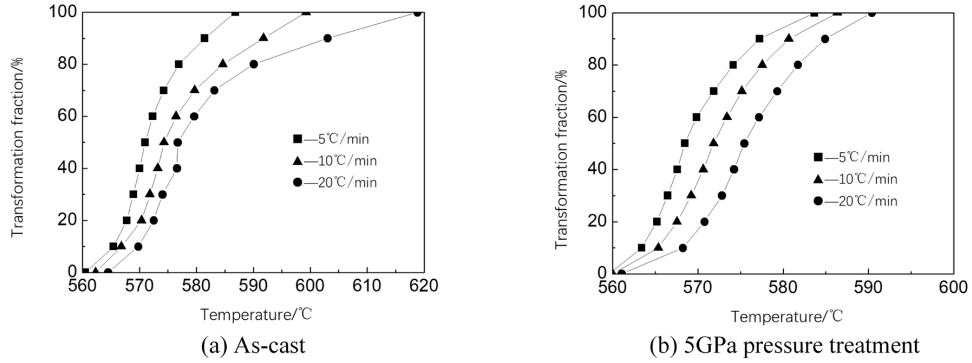
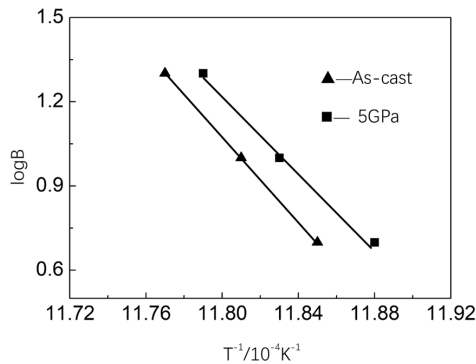
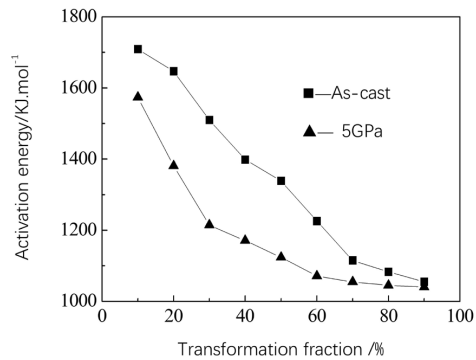


Fig. 5 - Plots of $\ln(B.T^{-2})\sim T^{-1}$ at DSC peak value of Cu-Al alloy before and after high pressure treatment under different heating rates

The phase transformation volume fraction (X_i) at different temperatures (T_i) of the samples with and without high pressure treatment can also be obtained from the DSC curves, as shown in Figure 6. Here X_i is calculated by the equation $X_i=S_i/S$, where S_i is the area of the endothermic peak on the DSC curves from the initial stage to a certain temperature (T_i) of the phase transformation, and S is the total area of the endothermic peak from the initial stage to the end of the phase transformation. Based on Figure 6, the relationship between $\log(B)$ and T^{-1} under different heating rates is further obtained in Figure 7, where the volume fraction for phase transformation is 50%. We see that the relationship of $\log(B)\sim T^{-1}$ is nearly linear which means that there is a linear relationship between $\log(B)$ and T^{-1} in the Deloy equation, and the slope is $K'=0.4567E_c/R$. Based on Figure 7, the slopes K' under two cases can be calculated by the least square method. Recall that the slope $K'=0.4567E_c/R$. Then the $\alpha+\gamma_2\rightarrow\beta$ phase transformation

Table 3 - Phase transformation temperature, duration and activation energy of Cu-Al alloy and $\text{Cu}_{61.13}\text{Zn}_{33.94}\text{Al}_{4.93}$ alloy before and after high pressure treatment.

Sample	Peak temperature		Transformation duration/s		Activation energy/ $\text{KJ}\cdot\text{mol}^{-1}$	
	As-cast	High pressure	As-cast	High pressure	As-cast	High pressure
Cu-Al alloy	571.16	568.11	365.08	261.32	1296.58	1174.85
$\text{Cu}_{61.13}\text{Zn}_{33.94}\text{Al}_{4.93}$ alloy	452.82	449.95	320.16	303.96	1106.03	843.07

**Fig.6** - Relationship between the transformation volume fraction and temperature before and after high pressure treatment at different heating rates**Fig.7** - Plots of $\log(B)\sim T^{-1}$ at 50% phase transformation volume fraction of Cu-Al alloy before and after high pressure treatment**Fig. 8** - Relationship between the phase transformation activation energy and the phase transformation volume fraction of Cu-Al alloy before and after high pressure treatment

activation energy (E_x) at the phase transformation volume fraction of 50% can be calculated by $E_x = K'R/0.4567$, that is 1338.65kJ/mol and 1123.39kJ/mol for As-cast and 5GPa, respectively. Similarly, we can obtain the phase

transformation activation energy under various volume fraction which is plotted in Figure 8. It indicates that the phase transformation activation energy is relatively higher at initial stage, and then decreases with increasing volume fraction. Thus, high pressure treatment can reduce the $\alpha+\gamma_2\rightarrow\beta$ phase transformation activation energy.

Note that the same method is used to calculate the phase transformation ($\beta'\rightarrow\beta$) parameters of $\text{Cu}_{61.13}\text{Zn}_{33.94}\text{Al}_{4.93}$ alloy before and after high pressure treatment²¹. The results show that high pressure treatment can reduce the phase transformation activation energy and temperature of $\text{Cu}_{61.13}\text{Zn}_{33.94}\text{Al}_{4.93}$ alloy, and further shorten the phase transformation duration. Moreover, high pressure treatment can refine the structure of $\text{Cu}_{61.13}\text{Zn}_{33.94}\text{Al}_{4.93}$ alloy. The results are in accordance with that in our experiment. We have further compared the results in Table 3.

3.4 Avrami exponent

The Avrami exponent (n) is an important kinetics parameter characterizing the phase transformation behavior such as nucleation and growth. The average Avrami exponent (n) of the Cu-Al alloy before and after high pressure treatment is given by $n = 2.5T_p^2(\Delta\tau_{FWTH}E_cR^{-1})^{-1}$, where $\Delta\tau_{FWTH}$ can be obtained from the DSC curves, and T_p and E_c have already been determined in the above. The relationship between the heating rate and Avrami exponent of Cu-Al alloy before and after high pressure treatment is illustrated in Figure 9. It shows that high pressure treatment can increase Avrami exponent (n), but the Avrami exponents (n) in both cases are less than 2. According to the range of Avrami exponent ($1 < n < 2$)^{22,23}, we can deduce that the $\alpha+\gamma_2\rightarrow\beta$ phase transformation of the Cu-Al alloy with and without high pressure treatment obeys one-dimensional growth mode characterized by gradually decreasing nucleation rate and diffusion-controlled crystal growth process. Therefore, high pressure treatment has less effect on the mechanism of $\alpha+\gamma_2\rightarrow\beta$ phase transformation.

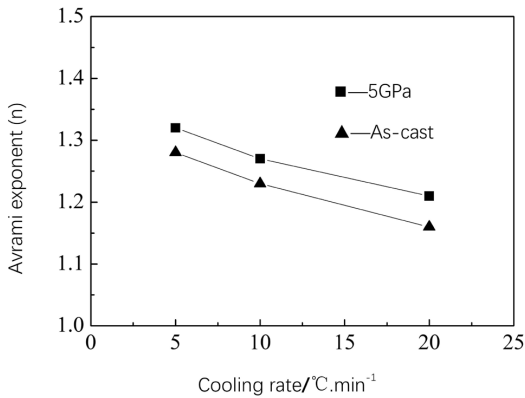


Fig. 9 - Relationship between the heating rate and Avrami exponent of Cu-Al alloy

3.5 Discussion

The $\alpha+\gamma_2\rightarrow\beta$ phase transformation process includes the formation and growth of crystal nucleus. The whole process is performed through the diffusion of atoms. With the increase of grain boundary, vacancies and dislocation in microstructure of Cu-Al alloy, more tunnels appear for the diffusion of Cu and Al atoms, which will then make the phase transformation much easier to be implemented. The fine grain microstructures obtained after high pressure treatment will increase the density of interface and the interfacial deficiency. Moreover, a lot of internal stress remaining in the alloy during heating process will cause plenty of lattice distortion and dislocations in the interior of grain. Note that the latter provides more favorable channel for the diffusion of copper and aluminum atoms. It will make the rearrangement of atoms easily to be achieved in the subsequent heating process. It will also reduce the activation energy and time for the phase transformation. All these are beneficial for the $\alpha+\gamma_2\rightarrow\beta$ phase transformation.

The experiments in this paper can only provide quantitative results for the effect of high pressure treatment on solid state phase transformation temperature, time and activation energy of the alloy, but it cannot display the mechanism and evolution during the solid state phase transformation in the alloy. When the endothermic peak in the DSC curve is very weak, or when the external factors have less impact on the phase transformation peak, there will be significant errors when adopting this experimental method. Note that the solid state phase transformation can be divided into two types: diffusion phase transformation and non-diffusion phase transformation. The internal friction will be generated during the phase transformation, thus introducing internal friction peak. Through the investigation of internal friction peak, information such as phase transformation type, phase transformation law and phase transformation degree, can be obtained²⁴. Therefore, it is interesting to combine the DSC method with the high-resolution TEM (HRTEM) image analysis methods and internal friction techniques. It has the potential to not only provide phase transformation parameters, such as phase transformation temperature and time, but also reveal the mechanism and evolution of phase transformation. It will be an effective method for the study of phase transformation in future.

4. Conclusion

1. High pressure treatment can decrease the $\alpha+\gamma_2\rightarrow\beta$ phase transformation temperature and shorten phase transformation duration, which is favorable to the $\alpha+\gamma_2\rightarrow\beta$ solid state phase transformation. Compared with no pressure treatment, the phase transformation peak temperature and the phase transformation duration of the Cu-Al alloy decrease by 2.7°C and 11.9s, respectively, after the processing of 5GPa pressure treatment and subsequent heating at the rate of 10°C·min⁻¹.
2. High pressure treatment can reduce the activation energy of the $\alpha+\gamma_2\rightarrow\beta$ solid phase transformation and elevate Avrami exponent during heating process, but it has less effect on the mechanism of the solid phase transformation.

5. References

1. Si NC, Zhao GQ, Yang DQ. Effects of mischmetal on mechanical properties of CuZnAl shape memory alloy. *Zhongguo Youse Jinshu Xuebao*. 2003;13(2):393-8.
2. Li RD, Cao XS, Qu YD. Effect of super high pressure on crystal structure and microstructure of ZA27 alloy. *Zhongguo Youse Jinshu Xuebao*. 2009;19(9):1570-4.
3. Wei ZJ, Wang ZL, Wang HW. Evolution of microstructures and phases of Al-Mg alloy under 4GPa high pressure. *J Mater Sci*. 2007;42(17):7123-8.
4. Liu YG, Xu L, Wang QF. Bulk α -Fe/Nd₂Fe₁₄B nanocomposite magnets prepared by the phase transition of amorphous Nd₂Fe₁₄B/Co₃Nb₁B₆ under high pressure. *Mater Lett*. 2008;62(23):3890-2.
5. Chen Y, Liu L, Wang YH, Liu JH, Zhang RJ. Microstructure evolution and thermal expansion of Cu-Zn alloy after high pressure heat treatment. *Trans Nonferrous Met Soc China*. 2011;21(10):2205-9.
6. Wang HY, Liu JH, Peng GR, Wang WK. Effects of high-pressure heat treatment on the solid-state phase transformation and microstructures of Cu_{61.13}Zn_{33.94}Al_{4.93} Alloys. *Chin Phys B*. 2010;19(9):096203-1-096203-6.
7. Liu YW, Liu L, Zhang W, Liu JH, Peng GR, Zhang RJ. Effect of high pressure heat treatment on microstructure and corrosion resistance of Brass. *Adv Mat Res*. 2011;194-196:1257-60.
8. Wu LL, Liu L, Liu JH, Zhang RJ. Effects of high pressure heat treatment on microstructure and micro-mechanical properties of Cu_{77.96}Al_{22.04} Alloy. *Mater Trans*. 2012;53(3):504-7.
9. Solomon ELS, Natarajan AR, Roy AM, Sundararaghavan V, Van der Ven A, Marquis EA. Stability and strain-driven evolution of β' precipitate in Mg-Y alloys. *Acta Mater*. 2019;166:148-57.
10. Natarajan AR, Solomon ELS, Puchala B, Marquis EA, Van der Ven A. On the early stages of precipitation in dilute MgNd alloys. *Acta Mater*. 2016;(108):367-79.
11. Levitas VI, Roy AM, Preston DL. Multiple twinning and variant-variant transformations in martensite: Phase-field approach. *Phys Rev B*. 2013;88:1-8.
12. Levitas VI, Roy AM. Multiphase phase field theory for temperature-and stress-induced phase transformations. *Phys Rev B*. 2015;91:174109-1-7.
13. Levitas VI, Roy AM. Multiphase phase field theory for temperature-induced phase transformations: formulation and application to interfacial phases. *Acta Mater*. 2016;105:244-57.
14. Wang HY, Chen Y, Liu JH, Wang WK. Effects of 3GPa high pressure treatment on the $\beta_1\rightarrow\alpha+\beta_2$ phase transition dynamics of TC4 titanium alloy. *Chinese Physics Letters*. 2013; 30(3):036202-1-3.

15. Yan C, Li Y, Liu J, Zhang R. Effect of 2GPa pressure treatment on the microstructure evolution of Cu-Zn alloy. *Mater Trans.* 2013;54(2):184-7.
16. Yan C, Li Y, Jian-Hua L, Rui-Jun Z. Effect of 4GPa pressure treatment on the solid state transformation kinetics of T8 Steel in following heating process. *Wuli Xuebao.* 2012;61(19):196203-1-6.
17. Liu JH, Li W, Chen Y. Effects of Zr on crystallization kinetics of Pr-Fe-B amorphous alloys. *Trans Nonferrous Met Soc China.* 2002;12(3):466-9.
18. Han ZL. Effects of high pressure treating on the phase transformation kinetics of austenite to pearlite in low carbon and low alloy steel. *J Mar Sci Eng.* 2007;1(1):61-6.
19. Jiang XY, Liu QS, Xu HB. The crystallization kinetics of amorphous Ti-rich NiTi film. *Journal of Functional Materials.* 2002;33(4):389-90.
20. Wang ZT. *Cu Alloys and it's working handbook.* Changsha: Central South University Press; 2002.
21. Wang HY, Liu JH, Peng GR, Wang WK. Effects of high-pressure heat treatment on the solid-state phase transformation and microstructures of $\text{Cu}_{61.13}\text{Zn}_{33.94}\text{Al}_{4.93}$ alloys. *Chin Phys B.* 2010;19(9):1-6.
22. Jiang XD, Zhang HW, Wen QY. The study of crystallization kinetics of CoNbZr amorphous soft magnetic thin films. *Journal of Functional Materials.* 2005;36(2):200-2.
23. Yan ZJ, Li JF, Wang HH. Study of the crystallization kinetics of Zr60Al15Ni25 bulk glassy alloy. *Wuli Xuebao.* 2003;52(8):1867-70.
24. Xu QP, Hao GL, Liu QP. Research progress and application of the internal friction technology. *Journal of Yanan University.* 2010;29(2):53-5.